

A Class of Sulfonamides with Strong Inhibitory Action against the α -Carbonic Anhydrase from *Trypanosoma cruzi*

Özlen Güzel-Akdemir,[†] Atilla Akdemir,^{*,‡} Peiwen Pan,[§] Alane B. Vermelho,^{||} Seppo Parkkila,[§] Andrea Scozzafava,[⊥] Clemente Capasso,[#] and Claudiu T. Supuran^{*,⊥,▽}

[†]Department of Pharmaceutical Chemistry, Faculty of Pharmacy, Istanbul University, 34116, Beyazit, Istanbul, Turkey

[‡]Department of Pharmacology, Faculty of Pharmacy, Bezmialem Vakif University, Vatan Cadd., Fatih, Istanbul, Turkey

[§]Institute of Biomedical Technology, Fimlab Ltd., School of Medicine and BioMediTech, University of Tampere and Tampere University Hospital, Medisiinärinkatu 3, 33520 Tampere, Finland

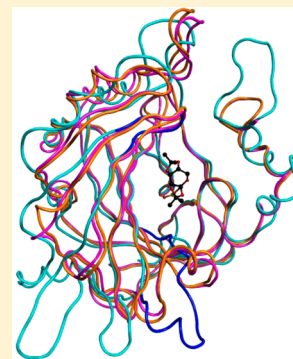
^{||}Laboratório Proteases de Microrganismos, Instituto de Microbiologia Paulo de Góes, Universidade Federal do Rio de Janeiro – UFRJ, CCS; Bloco I, Sala 32, Cidade Universitária, Av. Carlos Chagas Filho, 373, Ilha do Fundão; Rio de Janeiro R.J., Brazil

[⊥]Laboratorio di Chimica Bioinorganica, Polo Scientifico, Università degli Studi di Firenze, Room 188, Via della Lastruccia 3, 50019 Sesto Fiorentino (Florence), Italy

[#]Istituto di Biochimica delle Proteine – CNR, Via P. Castellino 111, 80131 Napoli, Italy

[▽]Sezione di Scienze Farmaceutiche, NEUROFARBA Department, Università degli Studi di Firenze, 50019 Sesto Fiorentino (Florence), Italy

ABSTRACT: *Trypanosoma cruzi*, the causative agent of Chagas disease, encodes for an α -carbonic anhydrase (CA, EC 4.2.1.1) possessing high catalytic activity (TcCA) which was recently characterized (Pan et al. *J. Med. Chem.* **2013**, *56*, 1761–1771). A new class of sulfonamides possessing low nanomolar/subnanomolar TcCA inhibitory activity is described here. Aromatic/heterocyclic sulfonamides incorporating halogeno/methoxyphenacetamido tails inhibited TcCA with K_i s in the range of 0.5–12.5 nM, being less effective against the human off-target isoforms hCA I and II. A homology model of TcCA helped us to rationalize the excellent inhibition profile of these compounds against the protozoan enzyme, a putative new antitrypanosoma drug target. These compounds were ineffective antitrypanosomal agents in vivo due to penetrability problems of these highly polar molecules that possess sulfonamide moieties.



■ INTRODUCTION

Chagas disease affects more than 10 million people, mostly in South and Central Americas, and is spreading also in Europe and North America.¹ It is caused by the protozoan parasite *Trypanosoma cruzi*, and only two drugs are clinically used for its treatment, the nitroazoles, benznidazole and nifurtimox, which are not always effective in eradicating the chronic infection.²

As the carbonic anhydrases (CAs, EC 4.2.1.1)^{3–7} are metalloenzymes involved in a variety of physiologic and pathologic processes, in many types of organisms, we recently started to explore them as possible anti-infective drug targets.⁸ Indeed, representatives of the α - and or β -CA class have been investigated in pathogenic bacteria such as *Brucella* spp., *Mycobacterium tuberculosis*, *Streptococcus pneumoniae*, *Salmonella enterica* serovar Typhimurium, *Vibrio cholerae*, and *Helicobacter pylori*, as well as in the pathogenic fungi *Candida albicans*, *C. glabrata*, and *Cryptococcus neoformans*.⁸ Only one protozoan parasite has been investigated up until now for the presence and drugability of CAs, the malaria-provoking organism *Plasmodium falciparum*.⁹ It has also been observed that some sulfonamides with potent inhibitory activity against the enzyme

from this parasite showed effective antimalarial action in vivo.⁹ We thus investigated whether *T. cruzi* may also possess such enzymes encoded in its genome.

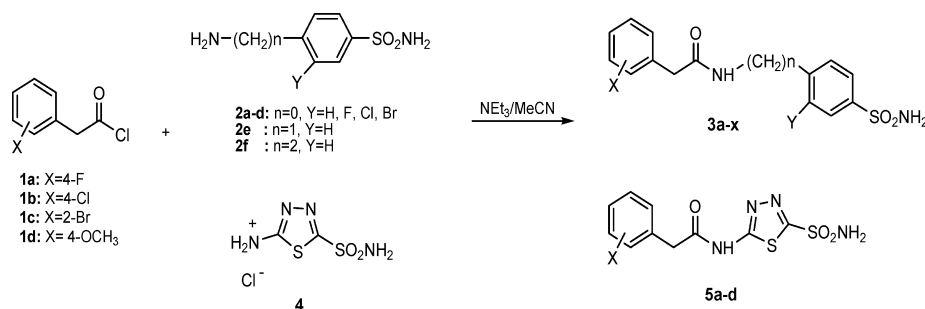
We have recently reported¹⁰ that an α -CA with very high catalytic activity is present in this organism, which was denominated TcCA, and that this enzyme is susceptible to inhibition by sulfonamides and thiols,¹⁰ two of the main classes of CA inhibitors (CAIs).^{3–7} Furthermore, some of the thiol CAIs also showed antitrypanosomal activity in vivo.¹⁰ However, the sulfonamides investigated previously were not effective in vitro TcCA inhibitors.¹⁰

The main class of CAIs is represented by the primary sulfonamides incorporating the SO₂NH₂ moiety which by coordinating to the metal ion from the enzyme active site impairs the formation of the zinc hydroxide nucleophile species of the enzyme, responsible for the hydration of CO₂ to bicarbonate, with a very high efficiency.^{3,4,11} A large number of such agents, mostly benzenesulfonamide derivatives, have been

Received: March 21, 2013

Published: July 1, 2013

Scheme 1. Preparation of the 4-[2-(Substituted phenyl)acetamido]benzenesulfonamides 3a–x and 5-[2-(Substituted phenyl)acetamido]-1,3,4-thiadiazole-2-sulfonamide Derivatives 5a–d



reported in recent years, as some of them were proven to possess strong antitumor activity in vivo, in animal models of the diseases, with effective inhibition of growth of both primary tumors and metastases,⁷ whereas other such agents show antiepileptic, antiobesity, and antiglaucoma activities and are clinically used.^{3,4,11}

Here we report the synthesis of a new class of sulfonamide derivatives obtained by the tail approach¹² and their subsequent testing for CA inhibition. These compounds potently inhibit TcCA and have a lower activity against the off-target human isoforms hCA I and II.

RESULTS AND DISCUSSION

Chemistry. Here we report a new class of sulfonamide derivatives obtained by the tail approach.¹² We have attached halogeno/methoxyphenacetamido tails to the molecules of aromatic or heterocyclic sulfonamides such as sulfanilamide, 3-halogenosulfanilamides, 4-aminomethyl/ethylbenzenesulfonamide, or 5-amino-1,3,4-thiadiazole-2-sulfonamide, as illustrated in Scheme 1. Reaction of the substituted phenacetyl chlorides **1a–d** with the amino-containing aromatic sulfonamides **2a–f** afforded the aromatic derivatives **3a–x**, whereas the same reaction involving the heterocyclic derivative **4** afforded the substituted 1,3,4-thiadiazole-2-sulfonamides **5a–d**. We have chosen various acyl chlorides **1a–d** to generate chemical diversity in this new class of sulfonamides, because we have observed previously that similar compounds, incorporating thienylacetamido, phenacetamido, and pyridinylacetamido tails, do show potent and isoform-selective inhibition profiles against some mammalian CA isoforms, such as CA VA and VB among others.¹³

Inhibition Data of TcCA and Human CA Isoforms I and II with the New Sulfonamides. The new sulfonamides **3** and **5**, as well as acetazolamide (AZ, 5-acetamido-1,3,4-thiadiazole-2-sulfonamide, a clinically used drug)^{3,4} have been tested in enzyme inhibition assays against TcCA (Table 1) using the stopped-flow, CO₂ hydrase Khalifah method.¹⁴ As seen from data of Table 1, AZ was a medium-potency CAI against TcCA (K_i of 61.6 nM),¹⁰ whereas the new sulfonamides reported here acted as highly potent low nanomolar or subnanomolar inhibitors of the protozoan enzyme, with K_i s in the range of 0.51–12.5 nM. The structure–activity relationship (SAR) for TcCA inhibition with the new sulfonamides reported here is rather straightforward:

- The 1,3,4-thiadiazole-2-sulfonamides **5a–d** were generally more effective CAIs compared to the benzenesulfonamides **3a–x** possessing similar scaffolds as tails. For example the 4-chloro-, 2-bromo-, and 4-methoxyphenyl-

Table 1. Inhibition Constants of Isozymes hCA I and II and TcCA with Sulfonamides 3a–x and 5a–d for the CO₂ Hydration Reaction (stopped-flow assay) at 20 °C¹⁴

no.	X, Y, n	K_i (nM) ^a			selectivity ratios	
		hCA I	hCA II	TcCA	hCA I/ TcCA	hCA II/ TcCA
3a	4-F, H, 0	102	7.9	8.5	12.0	0.9
3b	4-Cl, H, 0	346	104	2.7	128.1	38.5
3c	2-Br, H, 0	4.8	0.96	8.9	0.5	0.1
3d	4-MeO, H, 0	116	0.79	8.0	14.5	0.1
3e	4-F, F, 0	104	8.7	8.3	12.5	1.0
3f	4-Cl, F, 0	236	6.9	1.2	196.7	5.8
3g	2-Br, F, 0	8.6	1.9	1.6	5.4	1.2
3h	4-MeO, F, 0	106	0.78	4.1	25.9	0.2
3i	4-F, Cl, 0	254	9.5	7.0	36.3	1.4
3j	4-Cl, Cl, 0	9.8	7.3	7.7	1.3	0.9
3k	2-Br, Cl, 0	4.1	0.91	7.8	0.5	0.1
3l	4-MeO, Cl, 0	8.5	0.74	7.9	1.1	0.1
3m	4-F, Br, 0	246	8.9	9.0	27.3	1.0
3n	4-Cl, Br, 0	166	0.94	7.1	23.4	0.1
3o	2-Br, Br, 0	6.5	0.80	10.9	0.6	0.1
3p	4-MeO, Br, 0	8.7	0.69	7.2	1.2	0.1
3q	4-F, H, 1	109	9.3	3.7	29.5	2.5
3r	4-Cl, H, 1	109	0.81	12.5	8.7	0.1
3s	2-Br, H, 1	4.3	0.77	9.0	0.5	0.1
3t	4-MeO, H, 1	4.9	0.88	7.4	0.7	0.1
3u	4-F, H, 2	101	3.8	9.1	11.1	0.4
3v	4-Cl, H, 2	9.7	6.4	11.8	0.8	0.5
3w	2-Br, H, 2	8.2	0.72	3.3	2.5	0.2
3x	4-MeO, H, 2	3.7	0.81	7.5	0.5	0.1
5a	4-F, –, –	223	3.2	7.6	29.3	0.4
5b	4-Cl, –, –	4.9	0.70	0.95	5.2	0.7
5c	2-Br, –, –	7.6	0.70	0.83	9.2	0.8
5d	4-MeO, –, –	2.9	0.76	0.51	5.7	1.5
AZ	–	250	12	61.6	4.1	0.2

^aErrors in the range of 5–10% of the reported values (data not shown).

substituted 1,3,4-thiadiazolesulfonamides **5b–d** showed inhibition constants in the range of 0.51–0.95 nM, whereas most of the corresponding benzenesulfonamides incorporating the same tails were around 1 order of magnitude less efficient as TcCA inhibitors (Table 1)

- (ii) All tails present in these compounds (irrespective of whether the halogenophenacetamido possessed a fluorine, chlorine, or bromine in the 2- or 4-positions, or whether it was a 4-methoxyphenacetamido moiety) were equally effective in generating very strong TcCA inhibitors (Table 1).
- (iii) For the benzenesulfonamide derivatives **3a–x**, the fluorosulfanilamides **3e–h** were generally more inhibitory compared to the corresponding chlorosulfanilamides **3i–l**, the corresponding bromosulfanilamides **3m–p**, and the corresponding unsubstituted sulfanilamides **3a–d**, respectively, but the differences in activity were rather small. The increase in the spacer (n) between the benzenesulfonamide head and the tail (as in compounds **3q–t**, $n = 1$, and **3u–x**, $n = 2$) did not dramatically influence the TcCA inhibitory activity compared to the corresponding sulfanilamides **3a,b** ($n = 0$), Table 1.

The human isoforms hCA I and II were generally effectively inhibited by sulfonamides **3** and **5**, with K_{S} in the range of 2.9–346 nM (for hCA I) and of 0.70–104 nM (for hCA II). This is obviously not unexpected because most aromatic/heterocyclic sulfonamides possessing this type of substituted phenacetamido tail show relevant inhibitory activities against these two hCAs,¹³ which may be considered as off-targets. However, the reversible binding of a drug to the blood hCA I and II was recently shown to constitute a possibility to enhance the bioavailability of the drug and its slow release to organs not always reachable by sulfonamides.¹⁵ Inhibition of hCA I and II may be associated with side effects due to the ubiquity of these isoforms, but such phenomena are transient and are dose-dependent, being possible to find treatment windows at which the side effects are minimized.^{3,4,7}

The compounds in general showed selective inhibition of TcCA compared to hCA I. A subset of 17 compounds showed at least 5-fold selectivity toward TcCA over hCA I (Table 1). Compounds **3b** and **3f** showed the highest selectivity (more than 100 fold) against this isoform. However, 10 compounds showed similar inhibition values for hCA I and TcCA (hCA I/TcCA ratio: 0.5–1.3).

The compounds showed similar K_{S} for hCA II and TcCA (Table 1). Only three compounds showed selectivity toward TcCA, i.e., derivatives **3b** (38.5-fold), **3f** (5.8-fold), and **3q** (2.5-fold). Sulfonamide **3b** showed a marked selectivity toward TcCA compared to hCA I and hCA II. Replacement of the *p*-chlorine substituent by a *p*-fluorine (compound **3a**) or a *p*-methoxy substituent (compound **3d**) abolished the selectivity toward TcCA over hCA II, while it results in a ~10-fold drop in selectivity toward TcCA over hCA I (Table 1). Addition of a fluorine atom to the meta-position (with respect to the sulfamoyl moiety), to yield compound **3f**, increased the selectivity toward TcCA compared to hCA I, whereas it lowered the selectivity toward TcCA compared to hCA II (Table 1). Interestingly, adding a chlorine atom (compound **3j**) or a bromine atom (compound **3n**) instead of the fluorine lowered selectivity toward TcCA compared to both hCA I and hCA II (Table 1). Finally, increasing the spacer length between the amide bond and the aromatic ring (n in the general formula of the new sulfonamides reported here) with a methylene (compound **3r**) or ethylene moiety (compound **3v**) lowered the selectivity toward TcCA compared to both human CA isozymes (Table 1).

Docking Studies. To rationalize these results, and because no X-ray crystal structure is available so far for this new protozoan enzyme, we used a homology modeling strategy to understand the binding of sulfonamides **3a–x** and **5a–d** to TcCA. The homology model was built based on the *Neisseria gonorrhoeae* NgCA X-ray crystal structure (PDB: 1KOP),¹⁶ which shows 22.9% sequence identity to the TcCA. The three zinc-binding histidines and the two threonines near the zinc atom are conserved among NgCA and TcCA (His92, His94, His111, Thr177, and Thr178; NgCA numbering). In Figure 1,

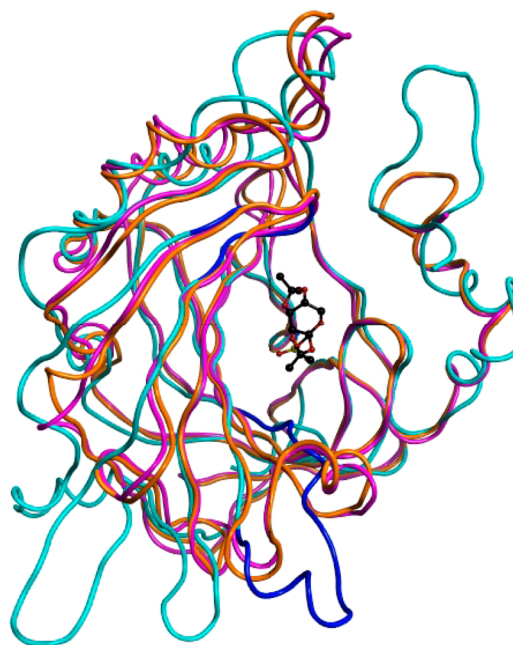


Figure 1. A homology model of TcCA based on the *Neisseria gonorrhoeae* enzyme (NgCA) X-ray crystal structure.¹⁶ hCA I (orange), hCA II (purple), and the homology model of TcCA (turquoise). The region where the backbone of TcCA has a different fold compared to hCA I and hCA II (Glu115–Ser122 and Thr183–Ala200 regions of TcCA) are depicted in dark blue (the sulfamate ligand topiramate is also shown).

a superposition of the obtained TcCA model with hCA I and II (as determined by X-ray crystallography)¹¹ is shown. The folding of TcCA is similar to that of hCA I and II (RMSD: 2.174 Å on α -atoms), but the protozoan enzyme possesses some extra loops (among which the Thr183–Ala200) which are absent in the mammalian enzymes. The counterpart of this loop is the Ser125–Val143 region of hCA I. The backbone of TcCA was folded outward from the binding pocket (compared to the other α -CA isozymes), and hence the binding pocket is larger (Figure 1) compared to those of the mammalian enzymes hCA I and II.^{17–20} The region between Glu115 and Ser122 in TcCA also had a different folding compared to hCA I and hCA II, being situated slightly closer toward the active site.

Sulfonamides **3a–x** and **5a–d** have been docked into the active sites of hCA I, hCA II, and TcCA, and all ligands were forced to position their sulfonamide groups in a way similar to that of topiramate in the hCA I crystal structure (PDB: 3LXE).¹⁷ Docking studies revealed that almost all these sulfonamides were able to adopt docking poses that allowed the formation of hydrogen bonds and cation– π interactions with Arg124 of TcCA. Furthermore, some of the ligands also

formed hydrogen bonds with Thr257. In addition, the ligands participated in hydrophobic interactions with Leu255. For example, compound 3b formed both a hydrogen bond and a cation- π interaction with the side chain of Arg124 from TcCA (Figure 2). In addition, the *p*-chlorine substituent of the ligand

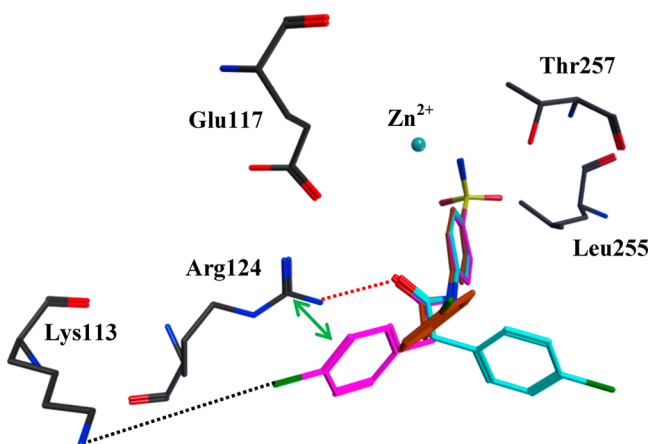


Figure 2. Docking poses of compound 3b (brown, magenta, and turquoise) within the active site of TcCA. The ligand forms hydrogen bonding to Arg124 (dashed red line). Also, the distance between the ligand phenyl moiety and the cationic group of Arg124 is close enough to form cation- π interaction (distance: ~ 3.5 Å; green double arrow; distance between atom CZ of Arg124 and the centroid of the ligand phenyl ring). The distance between the *p*-chlorine substituent of the ligand and the cationic nitrogen atom of Lys113 is ~ 5.62 Å (black dashed line), but this can decrease because of the Lys113 side chain flexibility.

could point in different directions, one of them toward the side chain of Lys113 and could probably form favorable electrostatic interactions with this residue. The distance between the Lys113 ϵ -nitrogen atom and the ligand chlorine atom was of 5.62 Å; however, this distance could decrease from the expected flexibility of Lys113. The residues Lys113, Arg124, and Thr257, which are important in the binding of ligands for TcCA, are on the other hand not present in hCA I and II (Table 2). In

Table 2. Amino Acid Residues of hCA I and II and TcCA Involved in the Binding of the Sulfonamide Inhibitors 3 and 5

hCA I (PDB: 3LXE)	hCA II (PDB: 3B4F)	TcCA (homology model)
Glu58	Arg58	Lys113
Asn69	Glu69	Arg124
Phe91	Ile91	Val155
Gln92	Gln92	Ser156
Ala121	Val121	Val179
Leu131	Phe131	different local fold
Thr199	Thr199	Thr256

addition, Glu69 is located in the hCA II binding site (its counterpart in TcCA is Arg124; see Table 2) close to the region where the chlorine substituent of the ligand was located, and this could cause unfavorable electrostatic interactions between the inhibitor and the enzyme.

Docking studies for hCA II showed that compounds 3 and 5 adopted an almost linear docking pose (see Figure 3 for a representative pose) and that hydrogen bonds were formed with the side chains of Gln92 and also occasionally with those

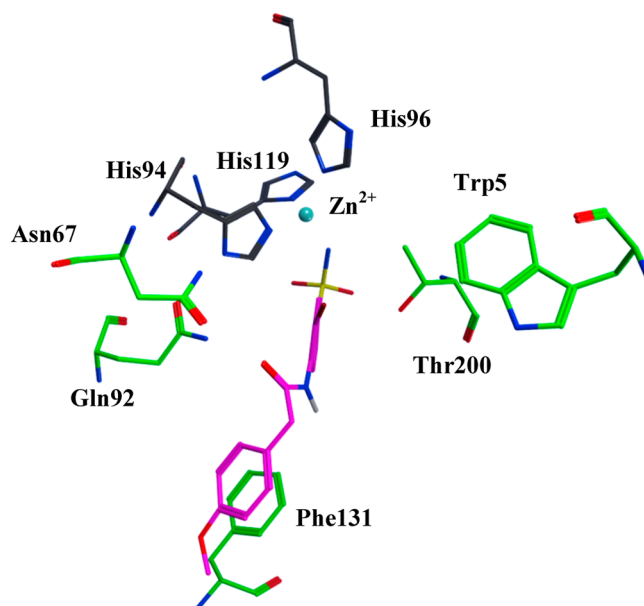


Figure 3. Docking poses of compound 3p (magenta) within the active site of hCA II. The methoxyphenyl moiety of the ligand forms hydrophobic stacking with Phe131. The residues that can form hydrogen bonds with several of the docked ligands are indicated in green. For clarity, Zn^{2+} and the zinc-binding residues His94, His96, and His119 are shown as well.

of Trp5 and Asn67. Interestingly, the compounds interacted with Phe131 through their halogenophenyl or methoxyphenyl moieties. This residue was shown (by means of X-ray crystallography)²² to form stackings (edge-to-face and face-to-face) with many sulfonamides and hence introduces a new stabilizing interaction with the bound inhibitors. Figure 3 shows the binding pose of compound 3p within the active site of hCA II to illustrate this interaction between the ligand phenyl moiety and Phe131. Phe131 is absent in the other two isozymes (Table 2). Its counterpart in hCA I is Leu131, whereas the corresponding backbone in TcCA is folded outward (the Thr183-Ala200 region of TcCA has a different backbone fold than the corresponding Ser125-Val143 region of hCA I and hCA II). In hCA I, Phe91 is present close to the region where Phe131 in hCA II is located. However, Phe91 (hCA I) is not available for stackings interactions with ligands because it seems to be shielded from the ligands by Gln92, Ala121, and Leu131.²²

Docking studies for hCA I also showed that compounds 3 and 5 adopt a near linear docking pose (data not shown). However, the absence of the Arg124 (TcCA) and Phe131 (hCA II) counterparts from hCA I could explain the higher K_I values for hCA I compared to hCA II and TcCA (Table 2).

The docking procedures did not always give clear and definitive explanations for the observed binding and/or inhibition data. Several reasons exist for this: (1) protein and binding pocket flexibility that are not taken into account by the docking procedures; (2) residues that do not directly contact the ligands can nevertheless have influences on their binding; (3) entropy effects that are not accurately taken into account in the docking procedures. Nevertheless, this docking study has resulted in a closer insight into the general inhibition data of the ligands reported here for hCA II (the presence of Phe131 that enables hydrophobic stacking interactions with the ligands) and TcCA (presence of Arg124 that enables cation- π

interactions and hydrogen bonding with the new sulfonamides) compared to hCA I. However, the homology model of TcCA and the crystal structure of NgCA superposed very well on their backbone atoms (1.591 Å, α -atoms) as shown in Figure 4.

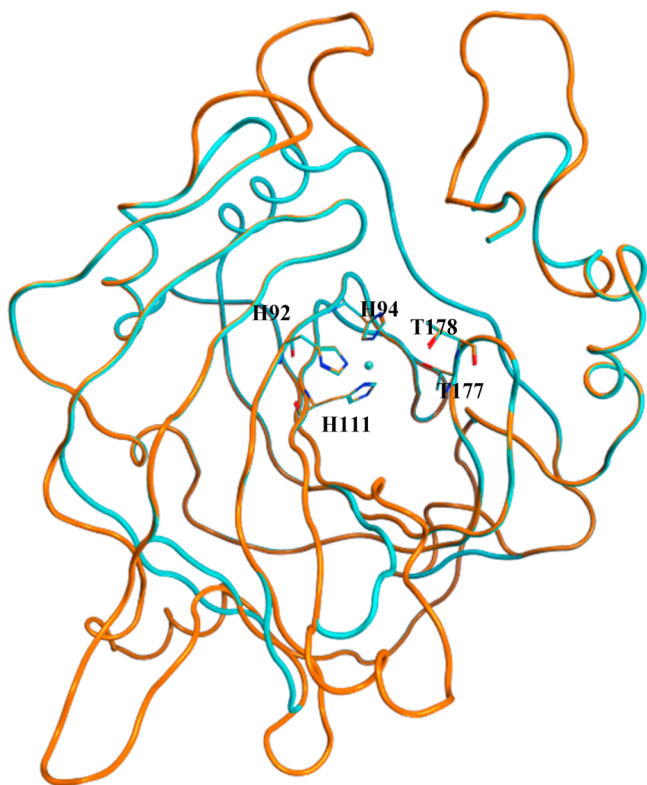


Figure 4. Overlay of the crystal structure of NgCA (turquoise) and the homology model of TcCA (brown) on their backbone α -atoms (RMSD: 1.591 Å). The three zinc-binding histidines and the two threonines are depicted for clarity (His92, His94, His111, Thr177, and Thr178; NgCA numbering) as well as the Zn^{2+} ions.

Obviously, the protozoan enzyme has some supplementary loops which are absent in the bacterial enzyme, but they are generally far away from the active site and this should influence the binding of inhibitors substantially.

In Vivo Inhibition Studies. Some of the most active in vitro CAIs, such as compounds **3f**, **3g**, **3w**, **5b**, **5g**, and **5d**, were investigated in vivo, for their antitrypanosomal effects, using epimastigotes of *T. cruzi* strains DM28 and Y, by the procedure of Rolon et al.²² The test compounds were used at concentrations of 256, 128, and 64 μM , and benznidazole **B** was used as standard drug. Although we have shown earlier that thiols acting as TcCA inhibitors do have antitrypanosomal effects in vivo,¹⁰ no such activity was detected for the compounds from the present paper (data not shown), when working in the concentration range of 64–256 μM CAI.

This lack of activity in vivo may be due to penetration problems of the sulfonamide compounds that, being highly polar molecules, have difficulties to cross biological membranes.^{23a} This problem was first encountered when the topical antiglaucoma sulfonamide CAIs were developed, as for more than 30 years it was impossible to obtain compounds effective via the topical route.^{23b–d} However, these efforts eventually led to the discovery of two clinically used drugs, dorzolamide and brinzolamide, when compounds with a balanced lipo- and hydrosolubility (as well as strong CA inhibitory properties)

were designed.²³ Both of these agents are highly effective and widely used as antiglaucoma agents.²⁴ A similar issue was encountered more recently for a sulfonamide with potent inhibitory action (in vitro) against the nematode α -CA from *Caenorhabditis elegans*.²⁵ Although low nanomolar compounds were obtained, they were ineffective in vivo as antinematode agents because of penetration problems. Thus, even if the in vivo data were negative with these sulfonamides, we estimate that our research may highlight the importance of this new antitrypanosomal drug target, TcCA, and the fact that focused drug design campaigns may lead to compounds which will also be active in vivo.

CONCLUSIONS

We report here a new class of sulfonamides which potentially inhibit TcCA, the enzyme from the protozoan that causes Chagas disease. An interesting SAR was evidenced for the inhibition of the protozoan and human off-target isoforms hCA I and II with these new sulfonamides. Homology modeling and docking studies allowed us to rationalize the particularly potent TcCA inhibition profile observed with some of these derivatives. As some CAIs were recently shown to possess antitrypanosomal activity in vivo, we estimate that this new class of inhibitors may allow interesting hints regarding the role of TcCA in the parasite life cycle and eventually be considered as lead molecules for new drug design studies against this disease. The new sulfonamides reported here were ineffective as antitrypanosomal agents probably because of their highly polar nature and inability to cross biological membranes to inhibit the parasite enzyme in vivo.

EXPERIMENTAL SECTION

Chemistry. All melting points were measured in open capillary tubes with Buchi 540 and are uncorrected. The compounds were checked for purity by TLC on silica gel HF₂₅₄ (E. Merck, Darmstadt, Germany). IR (KBr) spectra were recorded using a Perkin-Elmer 1600 FTIR spectrophotometer, and all values are expressed as ν_{max} cm^{-1} . ¹H NMR and ¹³C NMR (HSQC-2D) were recorded on Varian 300 MHz and Varian UNITY INOVA 500 spectrophotometers using DMSO-*d*₆ as solvent, and chemical shifts are given in ppm with TMS as a standard. All compounds were >99% pure as analyzed by HPLC.

General Procedure for the Preparation of Compounds 3 and 5. An amount of 5 mmol of aminosulfonamide was suspended/dissolved in 20–30 mL of anhydrous MeCN, and 0.78 mL (0.56 g, 5.5 mmol) of triethylamine was added under stirring. The mixture was cooled to 0–5 °C, and then a solution of 5 mmol of substituted phenylacetyl chloride in 3 mL of MeCN was added dropwise during 10 min (immediately a precipitate appeared). The reaction was stirred overnight or until a reasonable conversion was reached (TLC control). The solvent was evaporated in vacuum, and the resulting product was treated with 15–20 mL of cold water. The crude solid product was filtered, washed with water, and air-dried. The obtained compounds were further purified by recrystallization from ethanol.

4-[2-(4-Fluorophenyl)acetamido]benzenesulfonamide (3a). Yield 76%; mp 223–224 °C; IR (KBr) (ν , cm^{-1}), 1690 (C=O), 1149, 1325 (SO_2); ¹H NMR (DMSO-*d*₆, 500 MHz) δ (ppm): 3.67 (2H, s, CH_2CO), 7.13 (2H, t, $J = 8.78$ Hz, 4-FPh $\text{C}_{3,5}$ -H), 7.22 (2H, s, SO_2NH_2), 7.33–7.36 (2H, m, 4-FPh $\text{C}_{2,6}$ -H), 7.73 (4H, s, phenyl $\text{C}_{2,3,5,6}$ -H), 10.47 (1H, s, CONH); ¹³C NMR (HSQC-2D, DMSO-*d*₆, 125 MHz) δ (ppm): 42.93 (CH_2CO), 115.71 (d, $J_{\text{C,F}} = 21.08$ Hz, 4-FPh C_3 , C_5), 119.39 (Ph C_3 , C_5), 127.38 (Ph C_2 , C_6), 131.74 (d, $J_{\text{C,F}} = 8.14$ Hz, 4-FPh C_2 , C_6), 132.39 (4-FPh C_1), 139.09 (Ph C_1), 142.70 (Ph C_4), 161.86 (d, $J_{\text{C,F}} = 242.5$ Hz, 4-FPh C_4), 170.28 (CONH).

4-[2-(4-Chlorophenyl)acetamido]benzenesulfonamide (3b). Yield 90%; mp 231–232 °C; IR (KBr) (ν , cm^{-1}), 1670 (C=O), 1154, 1333 (SO_2); ¹H NMR (DMSO-*d*₆, 300 MHz) δ (ppm): 3.72 (2H, s,

CH₂CO), 7.26 (2H, s, SO₂NH₂), 7.39 (4H, d, *J* = 5.10 Hz, 4-ClPh C_{2,3,5,6}-H), 7.76 (4H, s, phenyl C_{2,3,5,6}-H), 10.53 (1H, s, CONH).

4-[2-(2-Bromophenyl)acetamido]benzenesulfonamide (3c). Yield 83%; mp 244–245 °C; IR (KBr) (ν , cm⁻¹), 1688 (C=O), 1153, 1351 (SO₂); ¹H NMR (DMSO-*d*₆, 300 MHz) δ (ppm): 3.93 (2H, s, CH₂CO), 7.27 (3H, d, *J* = 1.80 Hz, SO₂NH₂ and 2-BrPh C₄-H), 7.40–7.45 (2H, m, 2-BrPh C_{5,6}-H), 7.64 (1H, d, *J* = 6.30 Hz, 2-BrPh C₃-H), 7.78 (4H, d, *J* = 4.50 Hz, phenyl C_{2,3,5,6}-H), 10.60 (1H, s, CONH).

4-[2-(4-Methoxyphenyl)acetamido]benzenesulfonamide (3d). Yield 82%; mp 210–211 °C; IR (KBr) (ν , cm⁻¹), 1673 (C=O), 1154, 1331 (SO₂); ¹H NMR (DMSO-*d*₆, 300 MHz) δ (ppm): 3.63 (2H, s, CH₂CO), 3.75 (3H, s, CH₃O), 6.92 (2H, d, *J* = 6.60 Hz, 4-CH₃Oph C_{3,5}-H), 7.27 (4H, s, SO₂NH₂ and 4-CH₃Oph C_{2,6}-H), 7.77 (4H, s, phenyl C_{2,3,5,6}-H), 10.47 (1H, s, CONH).

4-[2-(4-Fluorophenyl)acetamido]-3-fluorobenzenesulfonamide (3e). Yield 81%; mp 196–198 °C; IR (KBr) (ν , cm⁻¹), 1673 (C=O), 1150, 1340 (SO₂); ¹H NMR (DMSO-*d*₆, 300 MHz) δ (ppm): 3.80 (2H, s, CH₂CO), 7.19 (2H, t, *J* = 8.40 Hz, 4-FPh C_{3,5}-H), 7.32–7.49 (4H, m, SO₂NH₂ and 4-FPh C_{2,6}-H), 7.53 (1H, s, 3-FPh C₂-H), 7.61 (1H, s, 3-FPh C₆-H), 8.50 (1H, d, *J* = 4.80 Hz, 3-FPh C₅-H), 10.24 (1H, s, CONH).

4-[2-(4-Chlorophenyl)acetamido]-3-fluorobenzenesulfonamide (3f). Yield 65%; mp 218–219 °C; IR (KBr) (ν , cm⁻¹), 1672 (C=O), 1151, 1339 (SO₂); ¹H NMR (DMSO-*d*₆, 500 MHz) δ (ppm): 3.76 (2H, s, CH₂CO), 7.35 (2H, d, *J* = 2.93 Hz, 4-ClPh C_{2,6}-H), 7.37 (2H, s, 4-ClPh C_{3,5}-H), 7.39 (2H, s, SO₂NH₂), 7.62 (1H, d, *J* = 1.95 Hz, 3-FPh C₂-H), 8.13 (1H, d, *J* = 8.30 Hz, 3-FPh C₆-H), 8.43 (1H, d, *J* = 6.83 Hz, 3-FPh C₅-H), 10.20 (1H, s, CONH); ¹³C NMR (HSQC-2D, DMSO-*d*₆, 125 MHz) δ (ppm): 42.41 (CH₂CO), 113.90 (d, *J*_{C,F} = 22.00 Hz, 3-FPh C₂), 122.07 (3-FPh C₅), 124.02 (3-FPh C₆), 127.13 (d, *J*_{C,F} = 12.94 Hz, 3-FPh C₄), 128.94 (4-ClPh C₃, C₅), 131.76 (4-ClPh C₂, C₆), 135.23 (4-ClPh C₄), 135.30 (4-ClPh C₁), 141.83 (d, *J*_{C,F} = 3.36 Hz, 3-FPh C₁), 154.50 (d, *J*_{C,F} = 250.30 Hz, 3-FPh C₃), 170.24 (CONH).

4-[2-(2-Bromophenyl)acetamido]-3-fluorobenzenesulfonamide (3g). Yield 86%; mp 213–214 °C; IR (KBr) (ν , cm⁻¹), 1669 (C=O), 1149, 1339 (SO₂); ¹H NMR (DMSO-*d*₆, 300 MHz) δ (ppm): 4.00 (2H, s, CH₂CO), 7.25 (1H, t, *J* = 7.20 Hz, 2-BrPh C₄-H), 7.38 (2H, t, *J* = 7.20 Hz, 2-BrPh C_{5,6}-H), 7.44 (2H, s, SO₂NH₂), 7.63 (1H, d, *J* = 8.10 Hz, 2-BrPh C₃-H), 7.70 (1H, s, 3-FPh C₂-H), 8.20 (1H, d, *J* = 7.50 Hz, 3-FPh C₆-H), 8.51 (1H, d, *J* = 7.50 Hz, 3-FPh C₅-H), 10.29 (1H, s, CONH).

4-[2-(4-Methoxyphenyl)acetamido]-3-fluorobenzenesulfonamide (3h). Yield 55%; mp 149–150 °C; IR (KBr) (ν , cm⁻¹), 1674 (C=O), 1150, 1339 (SO₂); ¹H NMR (DMSO-*d*₆, 300 MHz) δ (ppm): 3.71 (2H, s, CH₂CO), 3.76 (3H, s, CH₃O), 6.90 (2H, d, *J* = 7.80 Hz, 4-CH₃Oph C_{3,5}-H), 7.26 (2H, s, 4-CH₃Oph C_{2,6}-H), 7.41 (2H, s, SO₂NH₂), 7.60 (1H, s, 3-FPh C₂-H), 8.18 (1H, d, *J* = 6.00 Hz, 3-FPh C₆-H), 8.46 (1H, d, *J* = 6.00 Hz, 3-FPh C₅-H), 10.08 (1H, s, CONH).

4-[2-(4-Fluorophenyl)acetamido]-3-chlorobenzenesulfonamide (3i). Yield 98%; mp 213–214 °C; IR (KBr) (ν , cm⁻¹), 1669 (C=O), 1161, 1335 (SO₂); ¹H NMR (DMSO-*d*₆, 500 MHz) δ (ppm): 3.78 (2H, s, CH₂CO), 7.15 (2H, t, *J* = 7.81 Hz, 4-FPh C_{3,5}-H), 7.36–7.39 (2H, m, 4-FPh C_{2,6}-H), 7.42 (2H, s, SO₂NH₂), 7.71 (1H, dd, *J* = 8.78, 1.95 Hz, 3-ClPh C₆-H), 7.87 (1H, d, *J* = 1.95 Hz, 3-ClPh C₂-H), 7.96 (1H, d, *J* = 8.78 Hz, 3-ClPh C₅-H), 9.87 (1H, s, CONH); ¹³C NMR (HSQC-2D, DMSO-*d*₆, 125 MHz) δ (ppm): 42.29 (CH₂CO), 115.75 (d, *J*_{C,F} = 21.08 Hz, 4-FPh C₃, C₅), 125.59 (3-ClPh C₆), 126.03 (3-ClPh C₅), 127.49 (3-ClPh C₂), 131.82 (d, *J*_{C,F} = 8.14 Hz, 4-FPh C₂, C₆), 132.33 (3-ClPh C₃), 132.36 (4-FPh C₁), 138.52 (3-ClPh C₁), 141.73 (3-ClPh C₄), 161.89 (d, *J*_{C,F} = 242.03 Hz, 4-FPh C₄), 170.47 (CONH).

4-[2-(4-Chlorophenyl)acetamido]-3-chlorobenzenesulfonamide (3j). Yield 60%; mp 242–243 °C; IR (KBr) (ν , cm⁻¹), 1665 (C=O), 1161, 1331 (SO₂); ¹H NMR (DMSO-*d*₆, 300 MHz) δ (ppm): 3.84 (2H, s, CH₂CO), 7.42 (4H, s, 4-ClPh C_{2,3,5,6}-H), 7.48 (2H, s, SO₂NH₂), 7.77 (1H, d, *J* = 7.80 Hz, 3-ClPh C₆-H), 7.91 (1H, s, 3-ClPh C₂-H), 8.00 (1H, d, *J* = 7.80 Hz, 3-ClPh C₅-H), 9.98 (1H, s, CONH).

4-[2-(2-Bromophenyl)acetamido]-3-chlorobenzenesulfonamide (3k). Yield 92%; mp 220–221 °C; IR (KBr) (ν , cm⁻¹), 1678 (C=O), 1162, 1324 (SO₂); ¹H NMR (DMSO-*d*₆, 300 MHz) δ (ppm): 4.01 (2H, s, CH₂CO), 7.25 (1H, t, *J* = 7.80 Hz, 2-BrPh C₄-H), 7.39 (2H, t, *J* = 7.80 Hz, 2-BrPh C_{5,6}-H), 7.47 (2H, s, SO₂NH₂), 7.65 (1H, d, *J* = 8.10 Hz, 2-BrPh C₃-H), 7.76 (1H, dd, *J* = 8.40, 2.10 Hz, phenyl C₆-H), 7.91 (1H, d, *J* = 2.10 Hz, phenyl C₂-H), 8.02 (1H, d, *J* = 8.40 Hz, phenyl C₅-H), 9.98 (1H, s, CONH).

4-[2-(4-Methoxyphenyl)acetamido]-3-chlorobenzenesulfonamide (3l). Yield 91%; mp 176–177 °C; IR (KBr) (ν , cm⁻¹), 1673 (C=O), 1164, 1335 (SO₂); ¹H NMR (DMSO-*d*₆, 300 MHz) δ (ppm): 3.72–3.80 (5H, m, CH₂CO and CH₃O), 6.93 (2H, d, *J* = 7.80 Hz, 4-CH₃Oph C_{3,5}-H), 7.31 (2H, d, *J* = 8.40 Hz, 4-CH₃Oph C_{2,6}-H), 7.48 (2H, s, SO₂NH₂), 7.75 (1H, d, *J* = 8.40 Hz, 3-ClPh C₆-H), 7.90 (1H, s, 3-ClPh C₂-H), 8.02 (1H, d, *J* = 8.40 Hz, 3-ClPh C₅-H), 9.84 (1H, s, CONH).

4-[2-(4-Fluorophenyl)acetamido]-3-bromobenzenesulfonamide (3m). Yield 77%; mp 154–155 °C; IR (KBr) (ν , cm⁻¹), 1658 (C=O), 1156, 1341 (SO₂); ¹H NMR (DMSO-*d*₆, 500 MHz) δ (ppm): 3.70 (2H, s, CH₂CO), 7.14 (2H, t, *J* = 7.32 Hz, 4-FPh C_{3,5}-H), 7.32 (1H, d, *J* = 7.81 Hz, 3-BrPh C₆-H), 7.36 (2H, s, SO₂NH₂), 7.38 (2H, td, *J* = 7.32, 1.95 Hz, 4-FPh C_{2,6}-H), 7.57 (1H, dd, *J* = 7.81, 0.98 Hz, 3-BrPh C₅-H), 7.64 (1H, d, *J* = 0.98 Hz, 3-BrPh C₂-H), 9.57 (1H, s, CONH); ¹³C NMR (HSQC-2D, DMSO-*d*₆, 125 MHz) δ (ppm): 42.78 (CH₂CO), 115.72 (d, *J*_{C,F} = 21.08 Hz, 4-FPh C₃, C₅), 121.90 (3-BrPh C₃), 127.75 (3-BrPh C₅), 128.68 (3-BrPh C₆), 131.77 (d, *J*_{C,F} = 8.14 Hz, 4-FPh C₂, C₆), 132.32 (4-FPh C₁), 132.60 (3-BrPh C₂), 136.81 (3-BrPh C₁), 144.20 (3-BrPh C₄), 161.84 (d, *J*_{C,F} = 242.03 Hz, 4-FPh C₄), 162.84 (CONH).

4-[2-(4-Chlorophenyl)acetamido]-3-bromobenzenesulfonamide (3n). Yield 99%; mp 214–215 °C; IR (KBr) (ν , cm⁻¹), 1661 (C=O), 1161, 1345 (SO₂); ¹H NMR (DMSO-*d*₆, 300 MHz) δ (ppm): 3.74 (2H, s, CH₂CO), 7.41 (4H, s, 4-ClPh C_{2,3,5,6}-H), 7.48 (2H, s, SO₂NH₂), 7.60 (1H, d, *J* = 8.40 Hz, 3-BrPh C₆-H), 7.80 (1H, d, *J* = 8.40 Hz, 3-BrPh C₅-H), 8.06 (1H, s, 3-BrPh C₂-H), 9.69 (1H, s, CONH).

4-[2-(2-Bromophenyl)acetamido]-3-bromobenzenesulfonamide (3o). Yield %; mp 158–159 °C; IR (KBr) (ν , cm⁻¹), 1661 (C=O), 1172, 1342 (SO₂); ¹H NMR (DMSO-*d*₆, 500 MHz) δ (ppm): 3.89 (2H, s, CH₂CO), 7.11 (1H, td, *J* = 7.81, 1.47 Hz, 2-BrPh C₄-H), 7.20 (1H, td, *J* = 7.81, 1.47 Hz, 2-BrPh C₅-H), 7.34 (2H, s, SO₂NH₂), 7.37 (1H, d, *J* = 7.32 Hz, 3-BrPh C₆-H), 7.44 (1H, dd, *J* = 8.83, 1.47 Hz, 2-BrPh C₆-H), 7.59 (1H, dd, *J* = 7.81, 0.97 Hz, 2-BrPh C₂-H), 7.62 (1H, dd, *J* = 6.83, 0.98 Hz, 3-BrPh C₅-H), 7.65 (1H, d, *J* = 0.98 Hz, 3-BrPh C₂-H), 9.57 (1H, s, CONH); ¹³C NMR (HSQC-2D, DMSO-*d*₆, 125 MHz) δ (ppm): 43.50 (CH₂CO), 125.29 (2-BrPh C₂), 127.42 (3-BrPh C₅), 127.64 (2-BrPh C₄), 128.38 (3-BrPh C₆), 128.69 (3-BrPh C₃), 129.60 (2-BrPh C₅), 132.89 (2-BrPh C₆), 133.04 (2-BrPh C₃), 133.34 (3-BrPh C₂), 135.70 (2-BrPh C₁), 136.22 (3-BrPh C₁), 136.88 (3-BrPh C₄), 168.84 (CONH).

4-[2-(4-Methoxyphenyl)acetamido]-3-bromobenzenesulfonamide (3p). Yield 89%; mp 148–149 °C; IR (KBr) (ν , cm⁻¹), 1666 (C=O), 1167, 1338 (SO₂); ¹H NMR (DMSO-*d*₆, 300 MHz) δ (ppm): 3.66 (2H, s, CH₂CO), 3.75 (3H, s, CH₃O), 6.92 (2H, d, *J* = 6.60 Hz, 4-CH₃Oph C_{3,5}-H), 7.31 (2H, d, *J* = 6.90 Hz, 4-CH₃Oph C_{2,6}-H), 7.47 (2H, s, SO₂NH₂), 7.65 (1H, d, *J* = 7.50 Hz, 3-BrPh C₆-H), 7.80 (1H, d, *J* = 7.50 Hz, 3-BrPh C₅-H), 8.05 (1H, s, 3-BrPh C₂-H), 9.50 (1H, s, CONH).

4-[2-(4-Fluorophenyl)acetamidomethyl]benzenesulfonamide (3q). Yield 69%; mp 156–157 °C; IR (KBr) (ν , cm⁻¹), 1636 (C=O), 1159, 1338 (SO₂); ¹H NMR (DMSO-*d*₆, 300 MHz) δ (ppm): 3.50 (2H, s, CH₂CO), 4.34 (2H, d, *J* = 5.40 Hz, NHCH₂), 7.15 (2H, t, *J* = 8.70 Hz, 4-FPh C_{3,5}-H), 7.28–7.36 (4H, m, SO₂NH₂ and 4-FPh C_{2,6}-H), 7.39 (2H, d, *J* = 7.80 Hz, phenyl C_{3,5}-H), 7.76 (2H, d, *J* = 8.10 Hz, phenyl C_{2,6}-H), 8.65 (1H, s, CONH).

4-[2-(4-Chlorophenyl)acetamidomethyl]benzenesulfonamide (3r). Yield 62%; mp 186–187 °C; IR (KBr) (ν , cm⁻¹), 1635 (C=O), 1155, 1342 (SO₂); ¹H NMR (DMSO-*d*₆, 300 MHz) δ (ppm): 3.51 (2H, s, CH₂CO), 4.33 (2H, d, *J* = 4.80 Hz, NHCH₂), 7.32 (4H, s, SO₂NH₂ and 4-ClPh C_{2,6}-H), 7.36–7.42 (4H, m, 4-ClPh C_{3,5}-H and

phenyl C_{3,5}-H), 7.76 (2H, d, *J* = 8.40 Hz, phenyl C_{2,6}-H), 8.66 (1H, s, CONH).

4-[2-(2-Bromophenyl)acetamidomethyl]benzenesulfonamide (3s). Yield 69%; mp 193–194 °C; IR (KBr) (ν , cm⁻¹), 1649 (C=O), 1153, 1341 (SO₂); ¹H NMR (DMSO-*d*₆, 300 MHz) δ (ppm): 3.67 (2H, s, CH₂CO), 4.34 (2H, d, *J* = 5.86 Hz, NHCH₂), 7.18 (1H, td, *J* = 7.81, 1.95 Hz, 2-BrPh C₄-H), 7.28 (2H, s, SO₂NH₂), 7.31 (1H, td, *J* = 7.81, 1.46 Hz, 2-BrPh C₅-H), 7.36 (1H, dd, *J* = 7.32, 1.95 Hz, 2-BrPh C₆-H), 7.43 (2H, d, *J* = 8.29 Hz, phenyl C_{3,5}-H), 7.57 (1H, dd, *J* = 7.81, 0.97 Hz, 2-BrPh C₂-H), 7.76 (2H, d, *J* = 7.32 Hz, phenyl C_{2,6}-H), 8.59 (1H, s, CONH); ¹³C NMR (HSQC-2D, DMSO-*d*₆, 125 MHz) δ (ppm): 42.67 (CH₂CO), 42.96 (NHCH₂), 125.14 (2-BrPh C₂), 126.32 (Ph C₂, C₆), 128.20 (Ph C₃, C₅), 128.27 (2-BrPh C₅), 129.38 (2-BrPh C₄), 132.79 (2-BrPh C₆), 132.96 (2-BrPh C₃), 136.30 (2-BrPh C₁), 143.31 (Ph C₁), 144.30 (Ph C₄), 169.72 (CONH).

4-[2-(4-Methoxyphenyl)acetamidomethyl]benzenesulfonamide (3t). Yield 56%; mp 176–177 °C; IR (KBr) (ν , cm⁻¹), 1626 (C=O), 1152, 1327 (SO₂); ¹H NMR (DMSO-*d*₆, 300 MHz) δ (ppm): 3.43 (2H, s, CH₂CO), 3.75 (3H, s, CH₃O), 4.34 (2H, s, NHCH₂), 6.90 (2H, d, *J* = 6.00 Hz, 4-CH₃Oph C_{3,5}-H), 7.21 (2H, d, *J* = 7.50 Hz, 4-CH₃Oph C_{2,6}-H), 7.33 (2H, s, SO₂NH₂), 7.40 (2H, d, *J* = 7.50 Hz, phenyl C_{3,5}-H), 7.76 (2H, d, *J* = 6.00 Hz, phenyl C_{2,6}-H), 8.58 (1H, s, CONH).

4-[2-(4-Fluorophenyl)acetamidoethyl]benzenesulfonamide (3u). Yield 50%; mp 150–151 °C; IR (KBr) (ν , cm⁻¹), 1630 (C=O), 1157, 1342 (SO₂); ¹H NMR (DMSO-*d*₆, 300 MHz) δ (ppm): 2.79 (2H, s, NHCH₂CH₂), 3.38 (2H, s, CH₂CO), 3.44 (2H, s, NHCH₂CH₂), 7.14 (2H, d, *J* = 8.70 Hz, 4-FPh C_{3,5}-H), 7.23 (2H, s, SO₂NH₂), 7.32–7.37 (4H, m, 4-FPh C_{2,6}-H and phenyl C_{3,5}-H), 7.74 (1H, d, *J* = 7.50 Hz, phenyl C_{2,6}-H), 8.14 (1H, s, CONH).

4-[2-(4-Chlorophenyl)acetamidoethyl]benzenesulfonamide (3v). Yield 52%; mp 168–169 °C; IR (KBr) (ν , cm⁻¹), 1629 (C=O), 1157, 1339 (SO₂); ¹H NMR (DMSO-*d*₆, 300 MHz) δ (ppm): 2.80 (2H, t, *J* = 6.00 Hz, NHCH₂CH₂), 3.40 (2H, s, CH₂CO), 3.44 (2H, s, NHCH₂CH₂), 7.25 (2H, s, SO₂NH₂), 7.33–7.39 (6H, m, 4-ClPh C_{2,3,5,6}-H and phenyl C_{3,5}-H), 7.75 (2H, d, *J* = 7.20 Hz, phenyl C_{2,6}-H), 8.18 (1H, s, CONH).

4-[2-(2-Bromophenyl)acetamidoethyl]benzenesulfonamide (3w). Yield 95%; mp 170–171 °C; IR (KBr) (ν , cm⁻¹), 1651 (C=O), 1153, 1328 (SO₂); ¹H NMR (DMSO-*d*₆, 300 MHz) δ (ppm): 2.84 (2H, t, *J* = 6.60 Hz, NHCH₂CH₂), 3.40 (2H, s, CH₂CO), 3.58 (2H, s, NHCH₂), 7.21 (1H, t, *J* = 6.00 Hz, 2-BrPh C₄-H), 7.33 (4H, s, SO₂NH₂ and 2-BrPh C_{5,6}-H), 7.43 (2H, d, *J* = 7.80 Hz, phenyl C_{3,5}-H), 7.60 (1H, d, *J* = 8.10 Hz, 2-BrPh C₃-H), 7.77 (2H, d, *J* = 7.80 Hz, phenyl C_{2,6}-H), 8.16 (1H, s, CONH).

4-[2-(4-Methoxyphenyl)acetamidoethyl]benzenesulfonamide (3x). Yield 90%; mp 156–157 °C; IR (KBr) (ν , cm⁻¹), 1623 (C=O), 1157, 1336 (SO₂); ¹H NMR (DMSO-*d*₆, 300 MHz) δ (ppm): 2.75 (2H, t, *J* = 7.32 Hz, NHCH₂CH₂), 3.26–3.30 (4H, m, CH₂CO and NHCH₂CH₂), 3.71 (3H, s, CH₃O), 6.83 (2H, dd, *J* = 6.84, 1.95 Hz, 4-CH₃Oph C_{3,5}-H), 7.09 (2H, dd, *J* = 6.83, 1.95 Hz, 4-CH₃Oph C_{2,6}-H), 7.27 (2H, s, SO₂NH₂), 7.32 (2H, d, *J* = 8.78 Hz, phenyl C_{3,5}-H), 7.70 (2H, dd, *J* = 8.29, 1.95 Hz, phenyl C_{2,6}-H), 8.01 (1H, t, *J* = 5.37 Hz, CONH); ¹³C NMR (HSQC-2D, DMSO-*d*₆, 125 MHz) δ (ppm): 35.40 (NHCH₂CH₂), 39.70 (NHCH₂CH₂), 42.22 (CH₂CO), 55.72 (4-OCH₃), 114.33 (4-CH₃Oph C₃, C₅), 126.32 (phenyl C₂, C₆), 128.95 (4-CH₃Oph C₁), 129.82 (phenyl C₃, C₅), 130.59 (4-CH₃Oph C₂, C₆), 142.70 (phenyl C₁), 144.37 (phenyl C₄), 158.58 (4-CH₃Oph C₄), 171.18 (CONH).

5-[2-(4-Fluorophenyl)acetamido]-1,3,4-thiadiazole-2-sulfonamide (5a). Yield 59%; mp 273–274 °C; IR (KBr) (ν , cm⁻¹), 1684 (C=O), 1168, 1375 (SO₂); ¹H NMR (DMSO-*d*₆, 300 MHz) δ (ppm): 3.91 (2H, s, CH₂CO), 7.19 (2H, d, *J* = 8.10 Hz, 4-FPh C_{3,5}-H), 7.39 (2H, s, 4-FPh C_{2,6}-H), 8.35 (2H, s, SO₂NH₂).

5-[2-(4-Chlorophenyl)acetamido]-1,3,4-thiadiazole-2-sulfonamide (5b). Yield 59%; mp 285–286 °C; IR (KBr) (ν , cm⁻¹), 1689 (C=O), 1170, 1372 (SO₂); ¹H NMR (DMSO-*d*₆, 300 MHz) δ (ppm): 3.91 (2H, s, CH₂CO), 7.37 (2H, d, *J* = 8.70 Hz, 4-ClPh C_{2,6}-H), 7.42 (2H, d, *J* = 8.70 Hz, 4-ClPh C_{3,5}-H), 8.35 (2H, s, SO₂NH₂).

5-[2-(2-Bromophenyl)acetamido]-1,3,4-thiadiazole-2-sulfonamide (5c). Yield 59%; mp 247–248 °C; IR (KBr) (ν , cm⁻¹), 1680 (C=O), 1179, 1359 (SO₂); ¹H NMR (DMSO-*d*₆, 300 MHz) δ (ppm): 4.11 (2H, s, CH₂CO), 7.29 (1H, t, *J* = 6.90 Hz, 2-BrPh C₄-H), 7.42–7.47 (2H, m, 2-BrPh C_{5,6}-H), 7.67 (1H, d, *J* = 7.50 Hz, 2-BrPh C₃-H), 8.37 (2H, s, SO₂NH₂).

5-[2-(4-Methoxyphenyl)acetamido]-1,3,4-thiadiazole-2-sulfonamide (5d). Yield 64%; mp 256–157 °C; IR (KBr) (ν , cm⁻¹), 1685 (C=O), 1166, 1359 (SO₂); ¹H NMR (DMSO-*d*₆, 300 MHz) δ (ppm): 3.72 (3H, s, CH₃O), 3.79 (2H, s, CH₂CO), 6.88 (2H, dd, *J* = 6.40, 1.83 Hz, 4-CH₃Oph C_{3,5}-H), 7.23 (2H, dd, *J* = 6.86, 1.83 Hz, 4-CH₃Oph C_{2,6}-H), 8.29 (2H, s, SO₂NH₂), 13.19 (1H, s, CONH); ¹³C NMR (HSQC-2D, DMSO-*d*₆, 125 MHz) δ (ppm): 41.26 (CH₂CO), 55.77 (4-OCH₃), 114.63 (4-CH₃Oph C₃, C₅), 126.67 (4-CH₃Oph C₁), 131.09 (4-CH₃Oph C₂, C₆), 159.07 (4-CH₃Oph C₄), 161.90 (C-thiadiazole), 165.15 (C-thiadiazole), 171.29 (CONH).

CA Inhibition Assay. An Applied Photophysics stopped-flow instrument was used for assaying the CA-catalyzed CO₂ hydration activity.¹ Phenol red (at a concentration of 0.2 mM) was used as indicator, working at the absorbance maximum of 557 nm, with 20 mM HEPES (pH 7.5) as buffer and 20 mM Na₂SO₄ (for maintaining constant ionic strength), following the initial rates of the CA-catalyzed CO₂ hydration reaction for a period of 10–100 s. The CO₂ concentrations ranged from 1.7 to 17 mM for the determination of the kinetic parameters and inhibition constants. For each inhibitor, at least six traces of the initial 5–10% of the reaction were used for determining the initial velocity. The uncatalyzed rates were determined in the same manner and subtracted from the total observed rates. Stock solutions of inhibitor (0.1 mM) were prepared in distilled-deionized water, and dilutions up to 0.01 nM were performed thereafter with the assay buffer. Inhibitor and enzyme solutions were preincubated together for 15 min to 6 h at room temperature (15 min) or 4 °C (6 h) prior to assay, to allow for the formation of the E–I complex. The inhibition constants were obtained by nonlinear least-squares methods using PRISM 3, as reported earlier,² and represent the mean from at least three different determinations. All CA isofoms were recombinant ones obtained in-house as reported earlier.^{3–6}

Construction of TcCA Homology Models. Homology models of TcCA were constructed using the crystal structure of *Neisseria gonorrhoeae* CA (ngCA, PDB: 1KOP, 1.90 Å) as a template. Ten models were constructed using the MOE software package (version 2010, CCG, Montreal, Canada), and the model with both the lowest RMSD value (C α -atoms and all residues) and lowest contact energy was chosen for further optimization. A steepest descent energy minimization procedure (MMFF94x forcefield) was performed using default settings and with constraints on all heavy backbone atoms, His158, His160, His177, Thr256 (TcCA numbering; analogue of Thr199 in hCA I), and Zn²⁺. Afterward, a second round of energy minimization was performed with similar settings but without any constraints. The protein model was saved as a mol2 file prior to docking procedures. The homology model of TcCA and the crystal structure of NgCA superpose well on their backbone atoms (1.591 Å, C α -atoms; supplementary Figure 4). The crystal structures of hCA I (PDB: 3LXE), hCA II (PDB: 3B4F) and the homology model of TcCA superpose well on their C α -atoms (RMSD: 2.174 Å for 256 residues). The backbone folding near the binding pocket is similar for all CA isozymes except for Thr183-Ala200 of TcCA (counterpart of Ser125-Val143 region of hCA I). Here the backbone of TcCA is folded outward from the binding pocket compared to the other CA isozymes, and hence the binding pocket is larger (as shown Figure 1). Also, the region between Glu115 and Ser122 of TcCA has a different fold compared to the hCA I and hCA II and is situated slightly closer toward the active site.

Preparation of Protein Crystal Structures. Crystal structures hCA I (PDB: 3LXE; 1.90 Å) and hCA II (PDB: 3B4F; 1.89 Å) were obtained from the protein databank. Only one protein chain (chain A) and its corresponding Zn²⁺ ion and ligand (CA inhibitor) was retained per PDB file, and all other protein chains, ions, buffer molecules, and water molecules were deleted. Hydrogen atoms and charges were

added to the protein using the protonate 3D tool of the MOE software package (version 2010, CCG, Montreal, Canada), and a steepest descent energy minimization was applied (MMFF94x forcefield). All proteins were superposed (including the TcCA homology model) on the hCA I structure using their C α -atoms (RMSD: 2.174 Å), and the proteins with and without the CAI ligands were saved as mol2 files.

Preparation of Ligand Files. Three-dimensional coordinates of compounds 3 and 5 were prepared using the MOE software package (version 2010, CCG, Montreal, Canada). Subsequently, all strong bases were protonated, all strong acids were deprotonated, and the ligands were energy minimized according to a steepest descent protocol (MMFF94x forcefield) and finally saved as a multi-mol2 file.

Docking Studies. Compounds 3 and 5 were docked into the hCA I and hCA II protein models as well as the TcCA homology model using the GOLD Suite docking package (version 5.1, CCDC, Cambridge, UK)²¹ and the ChemScore scoring function (25 docking per ligand). ChemScore was chosen because of its speed and correct prediction of the binding poses as observed in crystal structures in redocking experiments.²¹ The binding pocket was defined as all residues within 12 Å of the central carbon atom of the CA inhibitor topiramate (atom CAL of topiramate in complex with hCA-I; PDB: 3LXE). No restrictions were applied for the ligand conformations during the docking procedure except for the position of its sulfonamide scaffold. All compounds were forced to position their sulfonamide moieties in a way similar to that of topiramate in complex with hCA-I (PDB: 3LXE), and a hydrogen bond with Thr199 (or its counterparts in other CA isozymes) was also required (using the “scaffold constraints” and “protein HBond” tools in the GOLD docking program).

Several crystal structures of α -type CA isozymes in complex with structurally diverse inhibitors were investigated prior to the docking procedure, and all these inhibitors positioned their sulfonamide groups in a way very similar to that observed in the topiramate–hCA I (PDB: 3LXE) complex. Therefore, compounds 3 and 5 were docked into the active sites of hCA I, hCA II, and TcCA, and all ligands were forced to place their sulfonamide groups in a way similar to that of topiramate in the hCA I crystal structure (PDB: 3LXE). Therefore, all docked compounds interact through their sulfonamide tail with Thr199 and Zn²⁺ of hCA I and their counterparts in hCA II and TcCA.

In Vivo Antitrypanosomal Activity. A quantitative colorimetric assay using the oxidation–reduction indicator resazurin was employed to measure cytotoxicity of compounds 26–33 against two strains of *T. cruzi*.²² The method is based on the detection of colorimetric changes caused by the oxidation (blue) and reduction (pink) capabilities of the resazurin dye, as an indicator for metabolic cell function. The inoculum of *T. cruzi* epimastigotes, the resazurin concentration, and the incubation time of different inocula of parasites were as described previously. A log-phase culture ranging from 0.25 to 9 × 10⁶/mL was seeded in different culture tubes for 24 h at 28 °C. Epimastigotes were then seeded on 96-well microtiter plates (Sarstedt, Sarstedt, Inc.) at 200- μ L/well volumes and incubated for another 48 h at 28 °C. After the incubation, 20 μ L of various dilutions of resazurin solutions ranging from 0.5 to 3 mM for each inoculum was added, and the plates were returned to the incubator. To choose the optimal duration of incubation for cultures in the presence of resazurin solution, the plates were incubated for periods ranging from 1 to 6 h to allow optimal oxidation–reduction. The absorbance values were read by dual wavelength using an EL × 800 enzyme-linked immunosorbent assay (ELISA) reader (Bio-Tek Instruments Inc.) at 490 and 595 nm. Background was subtracted. All experiments were performed three times each in triplicate at concentrations of test compound of 256, 128, and 64 μ M. Benznidazole was used as standard drug.

AUTHOR INFORMATION

Corresponding Author

*E-mail: aakdemir@bezmialem.edu.tr, tel: +90 212 523 22 88 ext. 1142, fax: +90 212 621 75 78 (A.A.); tel: +39-055-457-3005, fax: +39-055-457-3385, e-mail: claudiu.supuran@unifi.it (C.T.S.).

Notes

The authors declare the following competing financial interest(s): A patent application with these compounds has been filed.

ACKNOWLEDGMENTS

This research was financed by two EU projects (Metoxia and Dynano) to CTS, by grants from the Academy of Finland, Sigrid Jusélius Foundation, and Competitive Research Funding of Tampere University Hospital (9N054) to S.P. and by Coordenação de Aperfeiçoamento Pessoal de Nível Superior (CAPES), Conselho Nacional de Desenvolvimento Científico e Tecnológico (MCT/CNPq), Fundação Carlos Chagas Filho de Amparo à Pesquisa do Estado do Rio de Janeiro (FAPERJ), to A.B.V.. We thank Alfonso Maresca for technical support.

ABBREVIATIONS USED

CA, carbonic anhydrase; hCA I, human carbonic anhydrase I; hCA II, human carbonic anhydrase II; TcCA, *Trypanosoma cruzi* carbonic anhydrase; NgCA, *Neisseria gonorrhoeae* carbonic anhydrase; CAI, carbonic anhydrase inhibitors; AZ, acetazolamide; K_i, inhibition constant

REFERENCES

- (1) Coura, J. R.; Borges-Pereira, J. Chagas disease. What is known and what should be improved: a systemic review. *Rev. Soc. Bras. Med. Trop.* **2012**, *45*, 286–296.
- (2) Salomon, C. J. First century of Chagas' disease: an overview on novel approaches to nifurtimox and benznidazole delivery systems. *J. Pharm. Sci.* **2012**, *101*, 888–894.
- (3) Supuran, C. T. Carbonic anhydrases: novel therapeutic applications for inhibitors and activators. *Nat. Rev. Drug Discovery* **2008**, *7*, 168–181.
- (4) Supuran, C. T. Carbonic anhydrase inhibitors. *Bioorg. Med. Chem. Lett.* **2010**, *20*, 3467–3474.
- (5) Carta, F.; Aggarwal, M.; Maresca, A.; Scozzafava, A.; McKenna, R.; Supuran, C. T. Dithiocarbamates: a new class of carbonic anhydrase inhibitors. Crystallographic and kinetic investigations. *Chem. Commun. (Cambridge, U. K.)* **2012**, *48*, 1868–1870.
- (6) Di Fiore, A.; Maresca, A.; Alterio, V.; Supuran, C. T.; De Simone, G. Carbonic anhydrase inhibitors: X-ray crystallographic studies for the binding of N-substituted benzenesulfonamides to human isoform II. *Chem. Commun. (Cambridge, U. K.)* **2011**, *47*, 11636–11638.
- (7) Neri, D.; Supuran, C. T. Interfering with pH regulation in tumours as a therapeutic strategy. *Nat. Rev. Drug Discovery* **2011**, *10*, 767–777.
- (8) Supuran, C. T. Bacterial carbonic anhydrases as drug targets: toward novel antibiotics? *Front Pharmacol.* **2011**, *2*, 34.
- (9) Krungkrai, J.; Scozzafava, A.; Reungprapavut, S.; Krungkrai, S. R.; Rattanajak, R.; Kamchonwongpaisan, S.; Supuran, C. T. Carbonic anhydrase inhibitors. Inhibition of *Plasmodium falciparum* carbonic anhydrase with aromatic sulfonamides: towards antimalarials with a novel mechanism of action? *Bioorg. Med. Chem.* **2005**, *13*, 483–489.
- (10) (a) Pan, P.; Vermelho, A. B.; Capaci Rodrigues, G.; Scozzafava, A.; Tolvanen, M. E.; Parkkila, S.; Capasso, C.; Supuran, C. T. Cloning, Characterization, and Sulfonamide and Thiol Inhibition Studies of an alpha-Carbonic Anhydrase from *Trypanosoma cruzi*, the Causative Agent of Chagas Disease. *J. Med. Chem.* **2013**, *56*, 1761–1771. (b) Capasso, C.; Supuran, C. T. Anti-infective carbonic anhydrase inhibitors: A patent and literature review. *Expert Opin. Ther. Pat.* **2013**, *23*, 693–704.
- (11) Alterio, V.; Di Fiore, A.; D'Ambrosio, K.; Supuran, C. T.; De Simone, G. Multiple binding modes of inhibitors to carbonic anhydrases: how to design specific drugs targeting 15 different isoforms? *Chem. Rev.* **2012**, *112*, 4421–4468.

- (12) Casini, A.; Scozzafava, A.; Mincione, F.; Menabuoni, L.; Ilies, M. A.; Supuran, C. T. Carbonic anhydrase inhibitors: water-soluble 4-sulfamoylphenylthioureas as topical intraocular pressure-lowering agents with long-lasting effects. *J. Med. Chem.* **2000**, *43*, 4884–4492.
- (13) Guzel, O.; Innocenti, A.; Scozzafava, A.; Salman, A.; Supuran, C. T. Carbonic anhydrase inhibitors. Aromatic/heterocyclic sulfonamides incorporating phenacetyl, pyridylacetyl and thienylacetyl tails act as potent inhibitors of human mitochondrial isoforms VA and VB. *Bioorg. Med. Chem.* **2009**, *17*, 4894–4899.
- (14) Khalifah, R. G. The carbon dioxide hydration activity of carbonic anhydrase. I. Stop-flow kinetic studies on the native human isoenzymes B and C. *J. Biol. Chem.* **1971**, *246*, 2561–2573.
- (15) Stander, B. A.; Joubert, F.; Tu, C.; Sippel, K. H.; McKenna, R.; Joubert, A. M. In vitro evaluation of ESE-15-ol, an estradiol analogue with nanomolar antimitotic and carbonic anhydrase inhibitory activity. *PLoS One* **2012**, *7*, e52205.
- (16) Huang, S.; Xue, Y.; Sauer-Eriksson, E.; Chirica, L.; Lindskog, S.; Jonsson, B. H. Crystal structure of carbonic anhydrase from *Neisseria gonorrhoeae* and its complex with the inhibitor acetazolamide. *J. Mol. Biol.* **1998**, *283*, 301–310.
- (17) Alterio, V.; Monti, S. M.; Truppo, E.; Pedone, C.; Supuran, C. T.; De Simone, G. The first example of a significant active site conformational rearrangement in a carbonic anhydrase-inhibitor adduct: the carbonic anhydrase I-topiramate complex. *Org. Biomol. Chem.* **2010**, *8*, 3528–3533.
- (18) Pacchiano, F.; Aggarwal, M.; Avvaru, B. S.; Robbins, A. H.; Scozzafava, A.; McKenna, R.; Supuran, C. T. Selective hydrophobic pocket binding observed within the carbonic anhydrase II active site accommodate different 4-substituted-ureido-benzenesulfonamides and correlate to inhibitor potency. *Chem Commun (Cambridge, U. K.)* **2010**, *46*, 8371–8373.
- (19) Parkkila, S.; Vullo, D.; Maresca, A.; Carta, F.; Scozzafava, A.; Supuran, C. T. Serendipitous fragment-based drug discovery: ketogenic diet metabolites and statins effectively inhibit several carbonic anhydrases. *Chem. Commun. (Cambridge, U. K.)* **2012**, *48*, 3551–3553.
- (20) Winum, J. Y.; Maresca, A.; Carta, F.; Scozzafava, A.; Supuran, C. T. Polypharmacology of sulfonamides: pazopanib, a multitargeted receptor tyrosine kinase inhibitor in clinical use, potently inhibits several mammalian carbonic anhydrases. *Chem. Commun. (Cambridge, U. K.)* **2012**, *48*, 8177–8179.
- (21) Jones, G.; Willett, P.; Glen, R. C.; Leach, A. R.; Taylor, R. Development and validation of a genetic algorithm for flexible docking. *J. Mol. Biol.* **1997**, *267*, 727–748.
- (22) Rolon, M.; Vega, C.; Escario, J. A.; Gomez-Barrio, A. Development of resazurin microtiter assay for drug sensibility testing of *Trypanosoma cruzi* epimastigotes. *Parasitol. Res.* **2006**, *99*, 103–107.
- (23) (a) Scozzafava, A.; Carta, F.; Supuran, C. T. Secondary and tertiary sulfonamides: a patent review (2008–2012). *Expert Opin. Ther. Pat.* **2013**, *23*, 203–213. (b) Mincione, F.; Scozzafava, A.; Supuran, C. T. The development of topically acting carbonic anhydrase inhibitors as antiglaucoma agents. *Curr. Top. Med. Chem.* **2007**, *7*, 849–854. (c) Masini, E.; Carta, F.; Scozzafava, A.; Supuran, C. T. Antiglaucoma carbonic anhydrase inhibitors: A patent review. *Expert Opin. Ther. Pat.* **2013**, *23*, 705–716. (d) Fabrizi, F.; Mincione, F.; Somma, T.; Scozzafava, G.; Galassi, F.; Masini, E.; Impagnatiello, F.; Supuran, C. T. A new approach to antiglaucoma drugs: carbonic anhydrase inhibitors with or without NO donating moieties. Mechanism of action and preliminary pharmacology. *J. Enzyme Inhib. Med. Chem.* **2012**, *27*, 138–147.
- (24) (a) Supuran, C. T. Carbonic anhydrase inhibitors: An Editorial. *Expert Opin. Ther. Pat.* **2013**, *23*, 677–679. (b) Supuran, C. T. Structure-based drug discovery of carbonic anhydrase inhibitors. *J. Enzyme Inhib. Med. Chem.* **2012**, *27*, 759–772. (c) Carta, F.; Supuran, C. T.; Scozzafava, A. Novel therapies for glaucoma: a patent review 2007–2011. *Expert Opin. Ther. Pat.* **2012**, *22*, 79–88.
- (25) (a) Hall, R. A.; Vullo, D.; Innocenti, A.; Scozzafava, A.; Supuran, C. T.; Klappa, P.; Mühlischlegel, F. A. *Mol. Biochem. Parasitol.* **2008**, *161*, 140–149. (b) Güzel, Ö.; Innocenti, A.; Hall, R. A.; Scozzafava, A.; Mühlischlegel, F. A.; Supuran, C. T. Carbonic anhydrase inhibitors. The nematode α -carbonic anhydrase of *Caenorhabditis elegans* CAH-4b is highly inhibited by 2-(hydrazinocarbonyl)-3-substituted-phenyl-1H-indole-5-sulfonamides. *Bioorg. Med. Chem.* **2009**, *17*, 3212–3215.